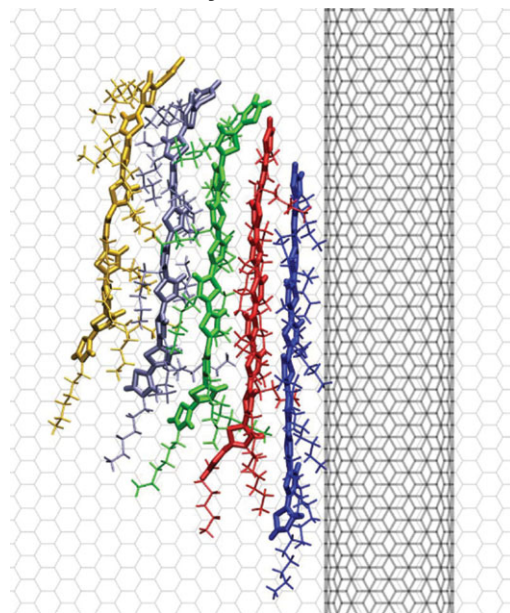


Synthesis and Characterization of Nanocomposites Based on Functional Regioregular Poly(3-hexylthiophene) and Multiwall Carbon Nanotubes^a

Florian Boon, Simon Desbief, Lorenzo Cutaia, Olivier Douhéret, Andrea Minoia, Benoît Ruelle, Sébastien Clément, Olivier Coulembier, Jérôme Cornil, Philippe Dubois, Roberto Lazzaroni*

New functionalized poly(3-hexylthiophene)s (P3HT) have been designed and synthesized with the aim of increasing the dispersion of carbon nanotubes (CNT) in solutions and in thin films of semiconducting polymers. Dispersion in solution has been assessed by sedimentation tests while the thin film morphology has been analyzed by TEM and AFM. Both the physisorption of P3HT chains (via pyrene end-groups) or their chemical grafting (onto amine functions generated on the CNT surface) lead to a much better dispersion in solution and in the solid. In thin films, P3HT fibrils are observed to arrange perpendicular to the CNT surface, which can be understood on the basis of molecular modeling simulations. Finally, the effect of dispersing those P3HT/CNT nanocomposites in bulk-heterojunction P3HT-based photovoltaic devices has been evaluated.



F. Boon, Dr. O. Coulembier, Dr. S. Clément, Dr. B. Ruelle,
Prof. Ph. Dubois

Laboratory of Polymeric and Composite Materials Center for
Innovation and Research in Materials and Polymers

F. Boon, Dr. S. Desbief, L. Cutaia, Dr. O. Douhéret, Dr. A. Minoia,
Dr. J. Cornil, Prof. R. Lazzaroni

Laboratory for Chemistry of Novel Materials Center for Innovation
and Research in Materials and Polymers

Fax: + 32 65 37 38 61;

E-mail: roberto@averell.umh.ac.be, or

olivier.coulembier@umons.ac.be

all at University of Mons-UMONS/Materia Nova, 20 Place du Parc,
B-7000 Mons (Belgium)

Introduction

Since their discovery in 1991, carbon nanotubes (CNT) have been extensively investigated for their unique electrical, mechanical, and optical properties.^[1] In terms of processing and incorporation into polymer materials, the main challenge of CNT chemistry is the dispersion and stabilization of CNT in different solvents and polymer matrices, which implies to overcome the nanotube aggregation due to strong van der Waals interactions between the sidewalls. For this purpose, two main strategies are proposed:

^a Supporting information for this article is available at the bottom of the article's abstract page, which can be accessed from the journal's homepage at <http://www.mrc-journal.de>, or from the author.

covalent and non-covalent CNT functionalization. The first one consists in grafting covalently reactive groups onto the nanotube sidewalls. This method can be carried out by treating CNTs with strong oxidizing reagents to form, for example, carboxylic acid groups. The main drawback is that such a treatment inevitably causes a disruption of the chemical structure of the CNT sidewalls and decreases dramatically the general properties.^[2] A new, gentler method to graft a functional group has been recently developed by Ruelle et al.;^[3] it uses a microwave plasma treatment to graft primary amines uniformly along the CNT sidewalls, while preserving the π -electronic structure and the properties of the CNTs.

The second approach is the non-covalent functionalization, which involves weak interactions such as van der Waals and π - π stacking to perturb the aggregation of the nanotubes and allow their dispersion.^[4] One major advantage is that the general properties of CNTs are preserved because the chemical structure of the sidewalls is not modified. To enforce that strategy, one can consider small conjugated molecules, like pyrene or porphyrin, which can interact with the sidewalls of CNT by π - π interactions. Such molecules have been grafted onto polymers, leading to a good dispersion of CNTs in solution and in bulk.^[5] Along the same line, conjugated polymers have been used to obtain a good dispersion of CNTs in polymer blends.^[6] In some cases, the two approaches have been combined, for instance with polyphenylacetylenes bearing pyrene side groups.^[7]

Besides assisting in the CNT dispersion, conjugated polymers are functional materials on their own, as they lie at the heart of organic electronic devices such as field-effect transistors or photovoltaic cells. Among those conjugated materials, regioregular poly(3-hexylthiophene) (P3HT) is of major interest, because of its outstanding electronic and optical properties and its good solubility in common organic solvents. It has also the capacity to self-assemble by π - π interactions to form crystalline nanowires, or fibrils, which favor charge carrier transport.^[8] The controlled synthesis of regioregular P3HT is most conveniently carried out by the Grignard Metathesis method (GRIM), as pioneered by McCullough and coworkers^[9] GRIM allows for the synthesis of P3HT with controlled regioregularity (>99%) and molecular weight (\overline{M}_n), narrow polydispersity index (PDI) (1.1–1.3), and defined end-groups (solely H/Br).^[10]

Blends containing P3HT and CNTs have been investigated in bulk heterojunctions for photovoltaic devices but the efficiencies of such devices are quite low compared to the classical P3HT:PCBM ([6,6]-phenyl-C₆₁-butyric acid methyl ester) blends.^[11] In order to optimize this type of blend, control over the morphology of the active layer is a primordial issue and one major problem is the poor dispersion of the CNTs in the conjugated matrix which

causes short circuits and decreases dramatically the performance of the devices.^[12,13]

Here we propose two strategies to increase the dispersion of multiwall carbon nanotubes (MWCNT) in solution and in P3HT thin films. We used a regioregular P3HT prepared by GRIM with well-known end-groups which can be modified into a formaldehyde function by a Vielsmeier–Haack reaction.^[14] We then used that function to form imine bonds by reaction with a primary amine present either on a pyrene molecule or on the MWCNT surface itself (Scheme 1). The pyrene end-functionalized P3HT can then interact with the CNT surface by non-covalent π - π stacking, while the reaction with the amine on the CNT leads to covalent P3HT grafting. Those new materials were first characterized in solution and by thermogravimetric analysis (TGA) to determine their stability. Then, a morphological study has been performed by transmission electron microscopy (TEM) and atomic force microscopy (AFM) on thin films of P3HT containing 1 wt.-% of MWCNT; the interpretation of the morphological data has been carried out with the assistance of molecular modeling simulations of the P3HT/CNT interface. Finally, photovoltaic cells incorporating those nanocomposites have been fabricated and tested. In the text, blends are noted with the components separated by “/” while covalently bound species are linked by “-”. For example, P3HT/MWCNT represents a simple blend between the polymer and the nanotubes whereas P3HT-MWCNT represents the covalently grafted system.

Experimental Part

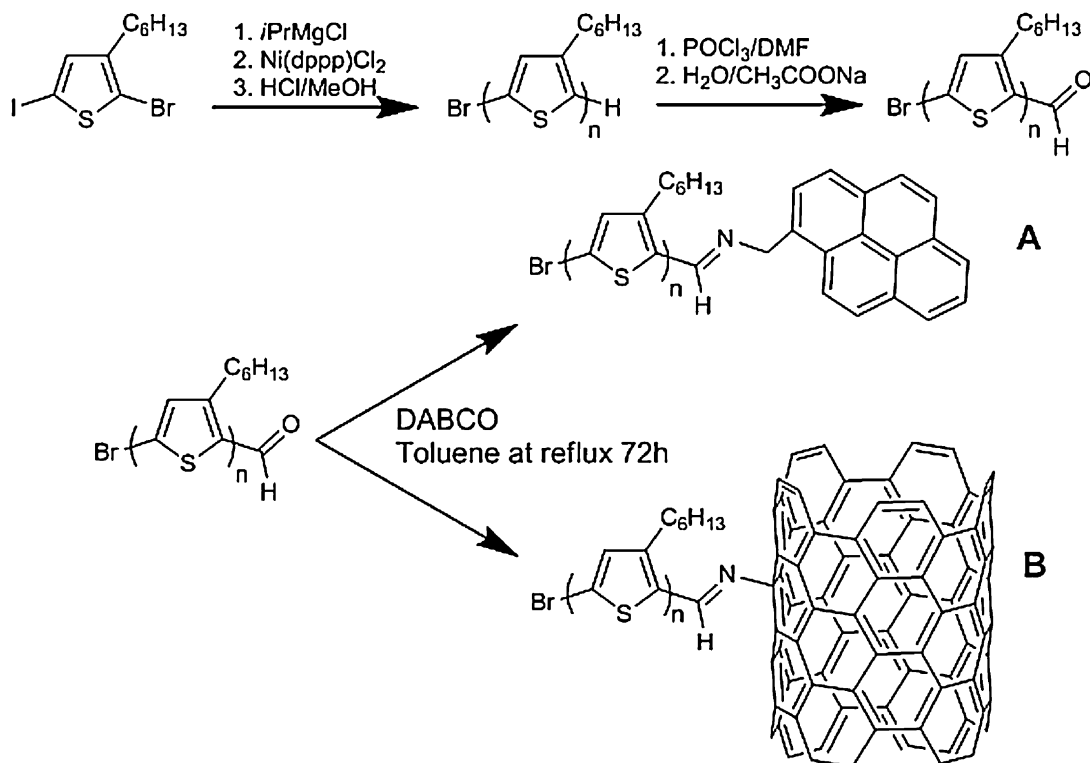
Functionalization of α -bromo ω -formyl Poly(3-hexylthiophene)

Br-P3HT-Pyrene (P3HT-Py)

Br-P3HT-C(O)H (the preparation is described in Supporting Information) ($\overline{M}_n = 9\,600$, PDI = 1.21) (250 mg, 0.026 mmol) was dissolved in anhydrous toluene (30 mL) under N₂. 1-Pyrenemethylamine (7.5 mg, 0.033 mmol) and 1,4-diazabicyclo[2.2.2]octane (20 mg, 0.18 mmol) were then added. The iminification reaction was carried out at reflux for 72 h. The polymer was recovered by precipitation in cold methanol. Yield = 85%; GPC analysis: $M_n = 9\,700\text{ g}\cdot\text{mol}^{-1}$; PDI = 1.21; IR (cm⁻¹): 819 (C–H aromatic out of plane), 1 620 (stretching of C=N group) and $I_{\text{sym}}/I_{\text{asym}} = 6$, characteristic of rr-HT-P3HT; ¹H-NMR (500 MHz, CDCl₃): 10 (s, 1H), 8.5 (s, 1H), 8.4–7.95 (pyrene: 9H), 6.98 (s, 1H), 5.58 (s, 2H), 2.80 (t, ³J = 7.5 Hz, 2H), 1.71 (quint, 2H), 1.34 (m, 6H), 0.91 (t, ³J = 6.4 Hz, 3H).

Br-P3HT-MWCNT (P3HT-MWCNT)

Br-P3HT-C(O)H ($\overline{M}_n = 9\,600$, PDI = 1.21) (100 mg, 0.01 mmol) was dissolved in anhydrous toluene (40 mL) under N₂ in the presence of MWCNT-NH₂ (100 mg) (Synthesis is described in Supporting Information). The mixture was sonicated for 15 min before adding



■ Scheme 1. Synthetic route to functional P₃HT for physisorption (A) or chemical grafting (B) on nanotubes.

1,4-diazabicyclo[2.2.2]octane (20 mg, 0.18 mmol). The reaction was carried out at reflux for 72 h and the product was recovered by precipitation in cold methanol.

Preparation of Carbon Nanotube Dispersions

P₃HT/MWCNT

P₃HT (25 mg) and MWCNT (25 mg) were added into 10 mL of THF. The mixture was sonicated for 30 min to allow disaggregation of the MWCNTs.

P₃HT-Py/MWCNT

P₃HT-Py (25 mg) and MWCNT (25 mg) were added into 10 mL of THF and the mixture was sonicated for 30 min.

P₃HT-MWCNT

50 mg of P₃HT covalently bonded to MWCNT by an imine bond were added into 10 mL of THF and sonicated for 30 min.

It should be noted that dispersions in chloroform gave similar results, while chlorobenzene appears to be less convenient because of the lower solubility of P₃HT in that solvent at room temperature.

Results and Discussion

Regioregular poly(3-hexylthiophene) (rrP₃HT) was synthesized using the GRIM polymerization method yielding an α -bromo-P₃HT with a predictable molecular weight ($\overline{M}_n = 9$

600 g · mol⁻¹) and a narrow molecular weight distribution ($\overline{M}_w/\overline{M}_n = 1.21$; see Supporting Information for structural analyses; Figure S1 and S2).^[15]

After quantitative formyl-dehydrogenation of the α -bromo-P₃HT protic end-group by a controlled and optimized Vilsmeier–Haack reaction,^[14] the polymer was converted to the desired product, α -bromo- ω -pyrene P₃HT (P₃HT-Py), by using 1-pyrenemethylamine in excess and 1,4-diazabicyclo[2.2.2]octane (DABCO) to drive the iminification (Scheme 1-A).

The success of the reaction has been attested by the disappearance of the vibrational band of the aldehyde group initially present at 1 650 cm⁻¹ and the appearance of a new vibrational band at 1 620 cm⁻¹ attributed to the imine function (see Figure S3 of Supporting Information). ¹H-NMR analysis also confirmed the iminification by the appearance of new signals at 5.58 and 8.5 ppm corresponding to the methylene (H_g) and methyne (H_f) protons of the imine bond, respectively (Figure S4 of Supporting Information). Based on the remaining signal (H_h), the iminification reaction has been estimated to be almost quantitative ($H_f/(H_f + H_h) \sim 90\%$). The same procedure has been used to perform the covalent grafting of P₃HT-C(O)H chains on MWCNT-NH₂ (Scheme 1 B).

To prove that the grafting effectively occurred and that the composites obtained are stable in solution, sedimentation tests have been performed. Three different solutions

have been prepared: a simple mixture of P3HT and MWCNTs (P3HT/MWCNT), a mixture of pyrene-functionalized P3HT and MWCNTs (P3HT-Py/MWCNT), and the covalently grafted system (P3HT-MWCNT). It is worth mentioning that the P3HT polymers used in those systems are all characterized by a \overline{M}_n of $9\,600\text{ g}\cdot\text{mol}^{-1}$, as determined by size exclusion chromatography. In a typical experiment, 25 mg of P3HT (or P3HT-Py) and 25 mg of MWCNTs were added in 10 mL of THF. In the case of P3HT-MWCNT, 50 mg of the material were added to 10 mL of THF. The solutions were then sonicated for 30 min. The comparative sedimentation evolutions of the MWCNT have been estimated by recording the H_d/H_t ratio vs. time with H_t , the height of total solution and H_d , the height of the sedimentation front (Figure 1 B). It is worth noting that the sedimentation evolution of pristine MWCNTs in THF was also measured as a reference. While after 1 h, the MWCNTs aggregate and leave a clear supernatant (Figure 1A), the physical blend of P3HT and CNTs (P3HT/MWCNT) shows a marked increase of the MWCNTs dispersion in solution, probably as a result of the π -stacking of the conjugated chains on the CNT surface. Upon covalent grafting of P3HT on MWCNT (P3HT-MWCNT), the stability of the dispersion is further improved compared to the stability of the simple physical blend, attesting for the efficiency of the covalent grafting process. Finally, the P3HT-Py compound appears to be extremely efficient in dispersing the CNTs, the supernatant remaining black after 24 h (Figure 1C). The sedimentation behavior therefore clearly depends on the functionalization, and it is affected by both the amount and the type of interactions between the P3HT and MWCNTs. Even if the direct covalent bonding of P3HT to MWCNTs is effective, the very low quantity of functionalizable amino groups on the surface of the MWCNTs (XPS analysis shows that the N/C ratio of the amino-modified CNTs is only around 1%) probably restricts the amount of P3HT around the nanotubes. For that reason, the sedimentation

rate is higher compared to that recorded for the P3HT-Py/MWCNT system. The association of the pyrene unit, which is known to physisorb on CNTs,^[5] and the P3HT chains allow to reach a point where no sedimentation is observed on the time scale of the experiment, probably due to π -interactions that efficiently disperse and stabilize the CNTs in the solution.

To quantify the content of MWCNTs in solution and to show any change in the degradation of the P3HT due to the interactions with CNTs, thermogravimetric analyses (TGA) were performed on all materials, including pristine MWCNTs. Samples were prepared by addition of 25 mg of P3HT to a corresponding amount of MWCNT in 100 mL of THF before sonication for 30 min. Compared to the sedimentation tests, an excess of THF has been used to allow for a better separation of the non-grafted P3HT from the MWCNTs. The solutions were then centrifuged at 4 000 rpm for 30 min at 15 °C and the supernatants were collected and evaporated. The residues were then dried at 100 °C overnight under reduced pressure and the TGA were performed under helium atmosphere from 25 to 900 °C using a $20\text{ }^\circ\text{C}\cdot\text{min}^{-1}$ heating rate. The pristine MWCNTs are still stable at 900 °C with negligible weight loss while P3HT has a maximum degradation temperature (MDT) around 480 °C and is completely degraded at 550 °C. Above such a temperature, the residues present, if any, indicate the quantity of MWCNT present in each system after centrifugation. The results are summarized in Table 1. In terms of residual CNT in the supernatant, the results are in good agreement with those obtained during the sedimentation tests; a higher stabilization of the CNTs in solution is observed when a functionalized P3HT is present (Entries B and C, Table 1). Concerning the MDT of P3HT, the results show that the presence of CNTs does not influence the degradation of the polymer significantly, in contrast to what has been observed in the case of the direct synthesis of P3HT by FeCl_3 .^[16] Sedimentations and TGA measurements

thus indicate that (i) a simple mixture of P3HT and MWCNT (P3HT/MWCNT) already shows an increase in stability of the CNTs in solution and (ii) the functionalization of P3HT further improves the stability of CNTs in solution in such a way that CNTs are still present in the supernatant after centrifugation.

To determine the influence of the functional P3HTs on the CNTs dispersion in a P3HT matrix, morphological studies were performed by TEM and AFM on the same three materials. The samples were prepared by drop casting a $0.25\text{ mg}\cdot\text{mL}^{-1}$ chlorobenzene solution with 1 wt.-% of MWCNT onto carbon-coated copper grids. Figure 2 shows typical TEM images

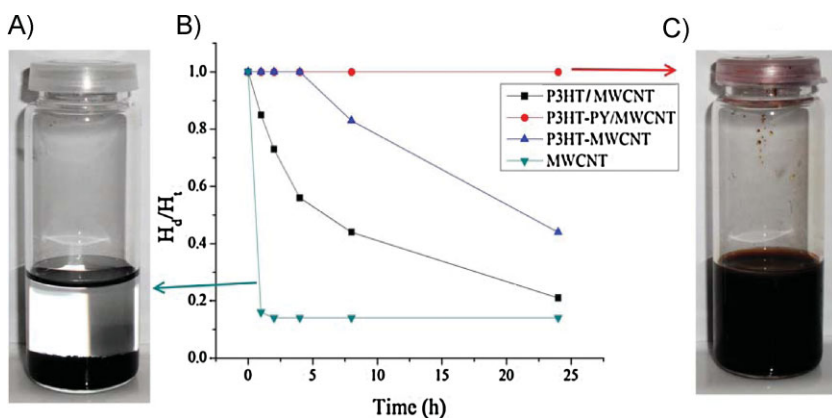


Figure 1. (A) Photograph of MWCNTs in THF after 2 h (B) Result of the sedimentation test for the three studied materials and pristine MWCNTs (C) Photograph of MWCNTs in a P3HT-Py solution in THF after 24 h.

Table 1. TGA performed on the nanocomposites under He from 25 to 900 °C with a heating rate of 20 °C · min⁻¹.

Sample	MDT	MWCNT
	°C	wt.-%
P3HT/MWCNT	479	0
P3HT-Py/MWCNT	467	5
P3HT-MWCNT	484	13

of the three materials. The dispersion of MWCNTs in the P3HT matrix is rather poor for the physical blend: large areas are totally devoid of CNTs, which often appear grouped in only a few locations, such as the one imaged in Figure 2A. On the contrary, the CNT distribution is much more homogeneous in the presence of the two functionalized materials; as a result, the CNTs are much better dispersed (Figure 2 B, C). These results confirm the ability to well disperse MWCNTs by using the covalent or non-covalent functionalization.

Atomic force microscopy in tapping mode (AFM-TM) was also performed on these materials. Thin films were prepared by drop casting 25 μL of the solutions onto 1 cm² ITO-coated glass substrates. P3HT films present a fibrillar morphology (Figure 3) with fibrils width of about 20 nm (See Figure S5 of Supporting Information), in good agreement with the molecular weight of the P3HT used, i.e. about 10 000 g · mol⁻¹, considering that those objects are built from π-stacked chains oriented perpendicular to the fibril axis.^[8] The AFM images suggest that the presence of MWCNTs does not globally disturb the organization of the P3HT chains into fibrils; the AFM data also show long bright protrusions in the height images, which are interpreted as being due to the presence of nanotubes surrounded by P3HT fibrils. The presence of the nanotubes as isolated objects, which confirms the quality of the dispersion, is better visualized in the phase images (see for instance image 3D), since the phase signal is more sensitive to the local mechanical properties.

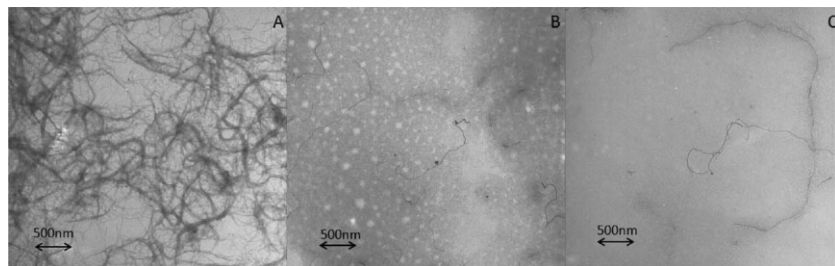


Figure 2. TEM images of P3HT/MWCNT (A); P3HT-Py/MWCNT (B); P3HT-MWCNT (C) prepared from 0.25 mg · mL⁻¹ chlorobenzene solutions with 1 wt.-% of MWCNTs.

In many locations, the P3HT fibrils in the vicinity of the CNTs appear to be arranged perpendicular to the nanotube sidewall, as also observed recently by Zhai and coworkers using TEM.^[6c] This is shown in the close-ups inserted in images 3B and 3D. We believe that this orientation, which is observed for both the covalent and non-covalent functionalization, originates from specific interactions between the polymer chains and the nanotubes. In order to rationalize this particular organization, molecular modeling simulations were carried out on model systems, consisting of an assembly of a few P3HT chains interacting with the surface of a single-wall nanotube (SWCNT). The simulations combined Molecular Mechanics and Molecular Dynamics approaches, with the aim of determining the supramolecular structure and assessing the energetics of the P3HT/CNT interface. Preliminary calculations were carried out on a single P3HT chain (with and without a pyrene end-group) interacting with an armchair SWCNT; the length of the chain was varied from ten to thirty monomer units and the diameter of the CNT from 1.36 to 5.42 nm (corresponding to values of the *n* index of SWCNTs of 10 and 40, respectively). Those calculations showed that the interaction energy (per monomer unit) is independent of the chain length and varies only slightly with the CNT diameter. When modeling the interface between the fibrils and the CNT, this allowed us to consider assemblies of the shorter chains interacting with the smaller tube, thus keeping the computational effort to a tractable level. The P3HT assemblies consisted of π-stacks of five to ten regioregular (3HT)₁₀ chains lying face-to-face. A single layer of graphene was added to the model, in order to reproduce the presence of the substrate in the actual system.

In the initial configuration, the P3HT assembly was brought in contact with the CNT, with both the π-stacking direction and the long axes of the conjugated backbones perpendicular to the axis of the tube, so as to reduce any bias due to the starting geometry. During the simulation, the assembly reorients, while maintaining its cohesion, in such a way that the first chain adsorbs flat on the CNT surface. The stacking direction thus becomes parallel to the nanotube axis. In the presence of the substrate, the polymer chains also tend to interact with the surface, thereby leading to the final structure shown in Figure 4. The driving force for the adsorption of the first chain “flat” on the surface of the CNT is the π-π interactions between the thiophene units and the π-system of the tube, as well as the CH-π interactions originating from the segments of the hexyl side groups that are in close proximity to the tube. Those two contributions lead to a stabilization energy of about 11 kcal · mol⁻¹ monomer unit for the

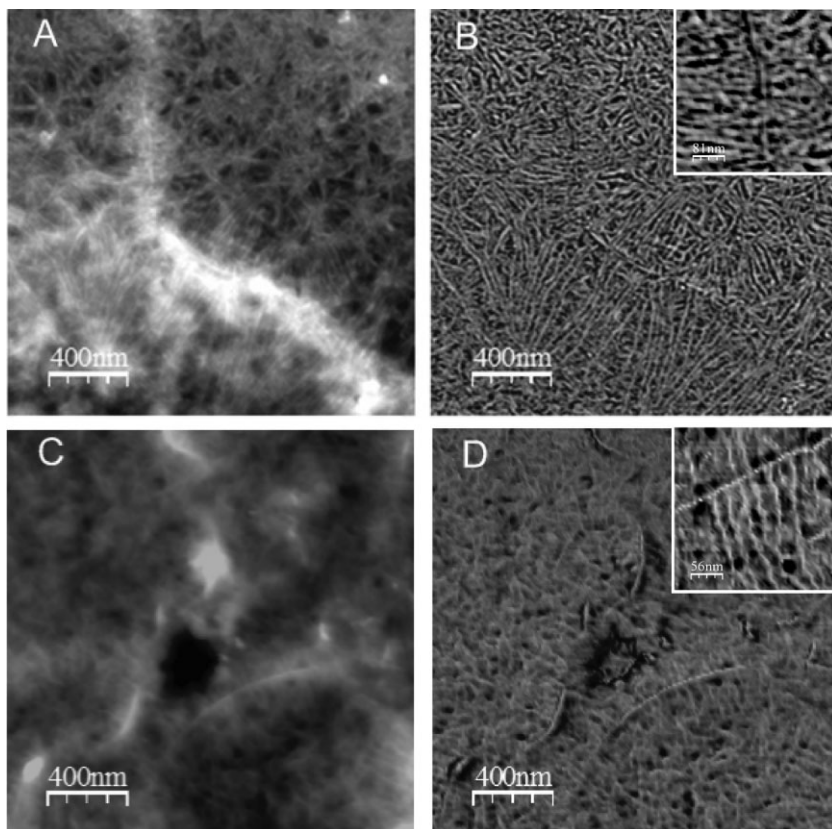


Figure 3. Tapping-mode AFM height (A) vertical scale 45 nm, C-vertical scale 70 nm) and phase (B,D) images of thin deposits of P₃HT-Py/MWCNT 1 wt.-% (A,B) and P₃HT-MWCNT 1 wt.-% (C,D). The insets in images B and D (scale bars: 80 and 56 nm, respectively) show close-ups on a single nanotube with P₃HT fibrils arranged perpendicular to it.

chain interacting with the CNT, with respect to the isolated partners. Figure 4 also indicates that the π -stacked structure of the P₃HT assembly is maintained and displays a staggered geometry in order to reduce the steric interactions between the sulfur atoms. The average intermolecular stabilization between P₃HT chains is $7.5 \text{ kcal} \cdot \text{mol}^{-1}$ monomer unit. The chain–CNT interactions thus appear to be stronger than the chain–chain interactions, which clearly favors adsorption on the tube surface. Note that when the P₃HT chain is end-functionalized with a pyrene unit, the global adsorption geometry on the CNT is very similar to that found for the non-functionalized chains (with the pyrene unit also adsorbing flat). However, the adsorption energy is significantly increased (by about 20% for a PY-(3HT)₁₀ chain), consistent with the better dispersion observed for the CNTs in the presence of that polymer. Finally, when the initial geometry involves a stack perpendicular to the CNT surface with the first chain adsorbed flat, no significant structural rearrangement occurs during the MD run, which further confirms the stability of that system.

These theoretical results thus point to the strong tendency for the conjugated chains to adsorb flat on the

CNT surface and to form π -stacks.^[17] One can therefore propose that the observed organization of the P₃HT fibrils around the nanotubes results from the initial adsorption of single P₃HT chains on the CNT surface in solution, followed by the gradual growth of the fibrils by π -stacking of other chains during the polymer deposition. Alternatively, short fibrils pre-formed in solution may adsorb on the nanotube surface with the first chain flat, thereby constituting a seed for further growth of the fibrils. The favorable interaction of the P₃HT chains with the CNT surface and the fact that the presence of a terminal pyrene unit further stabilizes that adsorbed chains are also quite consistent with the observations of the sedimentation tests and the TGA analysis.

Finally, the P₃HT-Pyrene/MWCNT system has been incorporated in P₃HT:PCBM photovoltaic devices. In practice, a suspension containing P₃HT, P₃HT-Py, and MWCNTs was prepared and then added with PCBM so that a 1:0.1:0.8 P₃HT:MWCNT:PCBM ratio was reached. That solution was then used to fabricate the devices, following the procedure described in the SI section. This mixed active layer was compared with a classical P₃HT:PCBM (1:0.8) blend. The corresponding J – V curves are shown in Figure S6 of the Supporting Information and the values of open-circuit voltage V_{oc} , current density J_{sc} , fill factor FF and power efficiency η are summarized in Table 2. The efficiency of the devices with nanotubes is significantly increased with respect to that of the classical devices. This increase appears to be related to an increase in the current density, which could be explained by a higher mobility of the charges induced by the presence of MWCNTs. In contrast, the V_{oc} does not change, which indicates that the dissociation of the excitons does not take place at the interfaces between P₃HT and MWCNT but rather at the P₃HT:PCBM interface.^[18]

Conclusion

In order to improve P₃HT-based photovoltaic devices, new P₃HT/CNT nanocomposites have been successfully prepared and characterized. Both the physisorption of P₃HT chains or their chemical grafting on the CNT surface lead to a much better dispersion of MWCNTs in solution and in the solid state. While dispersion in solution has been simply

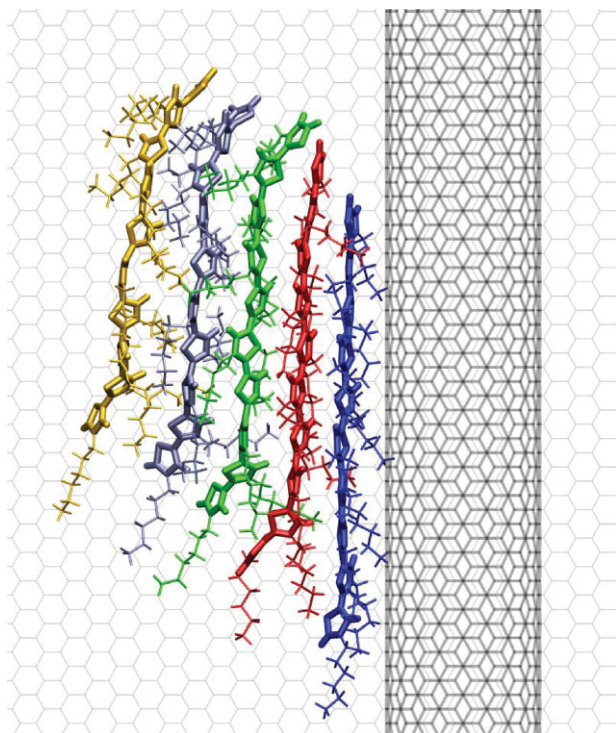


Figure 4. Snapshot extracted from an MD simulation of a ten-chain P3HT assembly interacting with a SWCNT (stick representation). For the sake of clarity, only the five chains closest to the nanotube are shown, each with a different color coding.

Table 2. Comparison of the device performances as obtained for P3HT:PCBM (1:0.8) blend and P3HT:P3HT-Py/MWCNT:PCBM (1:0.1:0.8) blend.

	P3HT:PCBM	P3HT:MWCNT: PCBM
V_{oc} (V)	0.57	0.58
J_{sc} ($\text{mA}\cdot\text{cm}^{-2}$)	6.80	8.83
FF (%)	56	52
η	2.17	2.64

assessed by sedimentation tests, thin film morphologies have been analyzed by TEM and AFM highlighting the formation of P3HT fibrils arranged perpendicular to the CNT surface, a process that has been understood and confirmed on the basis of molecular modeling simulations. Finally, the efficiency of the devices with CNTs has been demonstrated to be significantly increased with respect to that of classical devices.

Acknowledgements: This work has been supported by the European Commission and Région Wallonne FEDER program (Materia Nova), by the Interuniversity Attraction Pole program of the Belgian Federal Science Policy Office (PAI 6/27), by the SOLWATT program of Région Wallonne (SUNTUBE project), and by

FNRS-FRFC. F.B. is grateful to FRIA for a doctoral grant. O.C. and J.C. are Research Associate and Senior Research Associate of the FRS-FNRS, respectively.

Received: March 17, 2010; Revised: April 21, 2010; Published online: June 30, 2010; DOI: 10.1002/marc.201000183

Keywords: carbon nanotubes; dispersion; morphology; P3HT

- [1a] C. Thomsen, S. Reich, J. Maultzsch, "Carbon Nanotubes: Basic Concepts and Physical Properties", WILEY-VCH Verlag GmbH & Co, KGaA edition, Weinheim 2004; [1b] R. Andrews, D. Jacques, D. Qian, T. Rantell, *Acc. Chem. Res.* **2002**, *35*, 1008; [1c] S. Iijima, *Nature* **1991**, *354*, 56.
- [2] D. Tasis, N. Tagmatarchis, A. Bianco, M. Prato, *Chem. Rev.* **2006**, *106*, 1105.
- [3] B. Ruelle, S. Peeterbroeck, R. Gouttebaron, T. Godfroid, F. Monteverde, J.-P. Dauchot, M. Alexandre, M. Hecq, P. Dubois, *J. Mater. Chem.* **2007**, *17*, 157.
- [4] Y.-L. Zhao, J. F. Stoddart, *Acc. Chem. Res.* **2009**, *42*, 1161.
- [5] [5a] C. Ehli, G. M. A. Rahman, N. Jux, D. Balbinot, D. M. Guldi, F. Paolucci, M. Marcaccio, D. Paolucci, M. Melle-Franco, F. Zerbetto, S. Campidelli, M. Prato, *J. Am. Chem. Soc.* **2006**, *128*, 11222; [5b] X. Lou, R. Daussin, S. Cuenot, A.-S. Duwez, C. Pagnoulle, C. Detrembleur, C. Bailly, R. Jerome, *Chem. Mater.* **2004**, *16*, 4005; [5c] S. Meuer, L. Braun, T. Schilling, R. Zentel, *Polymer* **2009**, *50*, 154; [5d] D. M. Guldi, G. M. A. Rahman, F. Zerbetto, M. Prato, *Acc. Chem. Res.* **2005**, *38*, 871; [5e] W. Z. Yuan, J. W. Y. Lam, X. Y. Shen, J. Z. Sun, F. Mahtab, Q. Zheng, B. Z. Tang, *Macromolecules* **2009**, *42*, 2523.
- [6] [6a] M. Panhuis, A. Maiti, A. B. Dalton, A. van den Noort, J. N. Coleman, B. McCarthy, W. J. Blau, *J. Phys. Chem. B* **2003**, *107*, 478; [6b] S. Bhattacharyya, E. Kymakis, G. A. J. Amaratunga, *Chem. Mater.* **2004**, *16*, 4819; [6c] J. Liu, J. Zou, L. Zhai, *Macromol. Rapid Commun.* **2009**, *30*, 1387; [6d] J. Zou, H. Chen, A. Chunder, Y. Yu, Q. Huo, L. Zhai, *Adv. Mater.* **2008**, *20*, 3337; [6e] J. Zou, L. Liu, H. Chen, S. I. Khondaker, R. D. McCullough, Q. Huo, L. Zhai, *Adv. Mater.* **2008**, *20*, 2055; [6f] Y. K. Kang, O. S. Lee, P. Deria, S. H. Kim, T. H. Park, D. A. Bonnell, J. G. Saven, M. J. Therien, *Nano Lett.* **2009**, *9*, 1414.
- [7] W. Z. Yuan, J. Z. Sun, Y. Dong, M. Häussler, F. Yang, H. P. Xu, A. Qin, J. W. Y. Lam, Q. Zheng, B. Z. Tang, *Macromolecules* **2006**, *39*, 8011.
- [8] T. A. Skotheim, J. R. Reynolds, *Handbook of Conducting Polymers: Theory, synthesis, properties and characterization*, CRC Press, Boca Raton 2007.
- [9] R. S. Loewe, S. M. Khersonsky, R. D. McCullough, *Adv. Mater.* **1999**, *11*, 250.
- [10] [10a] R. Miyakoshi, A. Yokoyama, T. Yokozawa, *J. Am. Chem. Soc.* **2005**, *127*, 17542; [10b] E. E. Sheina, J. Liu, M. C. Iovu, D. W. Laird, R. D. McCullough, *Macromolecules* **2004**, *37*, 3526.
- [11] G. Dennler, M. C. Scharber, C. J. Brabec, *Adv. Mater.* **2009**, *21*, 1323.
- [12] [12a] E. Kymakis, I. Alexandrou, G. A. J. Amaratunga, *J. Appl. Phys.* **2003**, *93*, 1764; [12b] E. Kymakis, G. A. J. Amaratunga, *Appl. Phys. Lett.* **2002**, *80*, 112.
- [13] [13a] J. Geng, T. Zeng, *J. Am. Chem. Soc.* **2006**, *128*, 16827; [13b] M. Giulianini, E. R. Waclawik, J. M. Bell, M. De Crescenzi,

- P. Castrucci, M. Scarselli, N. Motta, *Appl. Phys. Lett.* **2009**, *95*, 013304; [13c] M. Giulianini, E. R. Waclawik, J. M. Bell, M. Scarselli, P. Castrucci, M. De Crescenzi, N. Motta, *Appl. Phys. Lett.* **2009**, *95*, 143116; [13d] B. K. Kuila, S. Malik, S. K. Batabyal, A. K. Nandi, *Macromolecules* **2007**, *40*, 278.
- [14] J. Liu, E. Sheina, T. Kowalewski, R. D. McCullough, *Angew. Chem., Int. Ed.* **2002**, *41*, 329.
- [15] M. Surin, O. Coulembier, K. Tran, J. De Winter, P. Leclère, P. Gerbaux, R. Lazzaroni, P. Dubois, *Org. Electron.* **2010**, *11*, 767.
- [16] V. Saini, Z. Li, S. Bourdo, E. Dervishi, Y. Xu, X. Ma, V. P. Kunets, G. J. Salamo, T. Viswanathan, A. R. Biris, D. Saini, A. S. Biris, *J. Phys. Chem. C* **2009**, *113*, 8023.
- [17] Our MD simulations indicate that the tendency for conjugated chains to wrap around CNTs, as reported previously (see, e.g., M. L. Colon et al., *J. Phys. Chem. B* **2008**, *112*, 12263 and Y. K. Kang et al., *Nano Lett.*, 2009, *9*, 1414) strongly depends on the diameter of the tube: while wrapping clearly occurs for single chains interacting with small SWCNTs (e.g., for diameters around 1.5 nm), this behavior tends to disappear for tubes with diameters around 5 nm, due to the reduced curvature, and is therefore not expected to play a major role in the actual systems, which contain MWCNTs with diameters around 10 nm.
- [18] S. Berson, R. deBettignies, S. Bailly, S. Guillerez, B. Jousseme, *Adv. Funct. Mater.* **2007**, *17*, 3363.